

Impacts of the New Carbon Fusion Cross Sections on Type Ia Supernovae

Kanji Mori^{1,2,3}, [★] Michael A. Famiano^{4,3}, Toshitaka Kajino^{1,2,3},
Motohiko Kusakabe^{3,1}, and Xiaodong Tang⁵

¹*National Astronomical Observatory of Japan, 2-21-1 Osawa, Mitaka, Tokyo, 181-8588 Japan*

²*Graduate School of Science, The University of Tokyo, 7-3-1 Hongo, Bunkyo-ku, Tokyo, 113-0033 Japan*

³*School of Physics and Nuclear Energy Engineering, Beihang University, 37 Xueyuan Road, Haidian-qu, Beijing 100083, China*

⁴*Department of Physics, Western Michigan University, Kalamazoo, Michigan 49008 USA*

⁵*Institute of Modern Physics, Chinese Academy of Science, Lanzhou, Gansu 730000, China*

Accepted XXX. Received YYY; in original form ZZZ

ABSTRACT

Type Ia supernovae (SNe Ia) are thought to be thermonuclear explosion of white dwarfs (WDs). Their progenitors are not well understood. One popular scenario is the double-degenerate (DD) scenario, which attributes SNe Ia to WD-WD binary mergers. The fates of the WD mergers depend on the rate of $^{12}\text{C}+^{12}\text{C}$ reaction. Recently, the $^{12}\text{C}+^{12}\text{C}$ cross sections have been measured and the analysis of the data using the Trojan Horse Method suggested that the astrophysical reaction rate is larger than conventional rates at astrophysical temperatures due to possible resonances. The resonance contribution results in a decrease of the carbon burning ignition temperature. Therefore accretion induced collapse occurs more easily and increases the birthrate of Galactic neutron stars with the contribution of the DD scenario to the SNe Ia rate becoming even smaller.

Key words: nuclear reactions – supernovae: general – white dwarfs – stars: evolution

1 INTRODUCTION

The carbon fusion reactions $^{12}\text{C}(^{12}\text{C}, \alpha)^{20}\text{Ne}$ ($Q_\alpha = 4.6$ MeV) and $^{12}\text{C}(^{12}\text{C}, p)^{23}\text{Na}$ ($Q_p = 2.2$ MeV) play the important roles in stellar evolution and explosive phenomena in the Universe (e.g. Iliadis 2008; Clayton 1968). The Gamow peak of these reactions is 1.5 MeV at a temperature of 5×10^8 K, which is typical in astrophysical environments. Experimentalists have pursued these reaction cross sections in the sub-Coulomb energy for many years, but the cross section below 2.1 MeV has not been reported with direct methods (Patterson, Winkler & Zaidins 1969; Spinka & Winkler 1974; Mazarakis & Stephens 1973; Kettner et al. 1977; High & Cujec 1977; Becker et al. 1981; Aguilera et al. 2006; Barrón-Palos et al. 2006; Spillane et al. 2007; Zickefoose 2010).

Many resonances which can be interpreted as molecular resonances (Imanishi 1968; Chiba & Kimura 2015) are suggested experimentally using indirect methods (Kawabata et al. 2013) above the $^{12}\text{C}+^{12}\text{C}$ threshold energy of the $^{24}\text{Mg}^*$ compound system. Cooper, Steiner & Brown (2009) developed the idea of a low energy resonance near the Gamow peak. They assumed a resonance at $E = 1.5$ MeV which does

not contradict the available cross section data and applied it to X-ray superbursts the ignition mechanism of which is still unclear. Bravo et al. (2011) and Bennett et al. (2012) considered similar low energy resonances in order to apply them to an accreting white dwarf (WD) and evolution of massive stars, respectively. These assumed resonances lead to significantly enhanced reaction rates compared with the standard non-resonant rate given by Caughlan & Fowler (1988) (hereafter CF88).

The resonance parameters proposed in the previous works were chosen so that resultant cross sections do not exceed the available cross section data at $E \approx 2.1$ MeV. However, it is unclear whether the chosen resonances are practically possible from the point of view of nuclear physics. In particular, the partial widths should be smaller than the Wigner limit (Teichmann & Wigner 1952; Clayton 1968).

Recently, the cross sections were measured for $E = 0.8$ MeV to 2.7 MeV using the Trojan Horse Method (Tumino et al. 2018a). Low-energy resonances which enhance the reaction rate by more than 25 times at $T \approx 5 \times 10^8$ K compared with CF88 were found. These can have significant impacts on a wide range of astrophysics.

In this paper, we focus on the impact of the enhanced reaction rates on WD-WD binary mergers. It is suggested

[★] E-mail: kanji.mori@nao.ac.jp

that they are progenitors not only of type Ia supernovae (SNe Ia) (Iben & Tutukov 1984; Webbink 1984) but also of short γ -ray bursts (e.g. Levan et al. 2006) and fast radio bursts (Kashiyama, Ioka & Mészáros 2013), though their evolutions and final fates are still under debate. The reaction rate of carbon fusion is the most important input in this system because the reaction chain begins from $^{12}\text{C}+^{12}\text{C}$ due to its small electric charge among all stable nuclei in the burning layers.

Keane & Kramer (2008) estimated birthrates of Galactic neutron stars (NSs) and pointed out that they exceed the Galactic core-collapse supernova (CCSN) rate. One possible solution for this birthrate problem is the existence of sources of NSs other than CCSNe. It has been pointed out that the carbon burning flame in a WD-WD merger can turn a carbon-oxygen (CO) WD into an oxygen-neon-magnesium (ONeMg) WD (Nomoto & Kondo 1991). The ONeMg WD cannot support its mass and collapses into a NS. This evolutionary path enhances the NS birthrates, therefore it is worthwhile to estimate an event rate for this path. The condition for carbon burning to ignite and evolve a CO WD into a NS depends on the $^{12}\text{C}+^{12}\text{C}$ reaction rate.

Here, we apply the new resonant carbon fusion reaction rate to the WD-WD mergers and discuss their fate in the context of the birthrate problem of Galactic NSs.

2 CONSTRAINT ON THE RESONANCES

The partial decay width Γ_C for the $^{12}\text{C}+^{12}\text{C}$ channel at astrophysically low energies $E < 2$ MeV is too far to reach both experimentally and theoretically because it is expected to be extremely small due to the Coulomb barrier between two carbons. Partial widths larger than the Wigner limit are practically impossible in terms of nuclear structure (e.g. Clayton 1968), therefore we adopt it as a conservative upper limit on the width:

$$\Gamma_C(E_R) = 2\gamma^2 P_C(E_R) = 2\gamma_W^2 P_C(E_R)\theta^2 < 2\gamma_W^2 P_C(E_R), \quad (1)$$

where P_C is the Coulomb penetration factor, E_R is the resonance energy, γ^2 is the reduced width, and $\gamma_W^2 = 3\hbar^2/2\mu a^2$ is the Wigner limit. Here, μ is the reduced mass and a is the channel radius. The partial widths are often parametrized by the dimensionless reduced width $\theta^2 = \gamma^2/\gamma_W^2$, i.e. $\theta^2 = 1$ is the Wigner limit.

Fig. 1 shows the upper limit of the resonance strength deduced from Eq. (1) and resonance parameters are the same as those adopted in the previous works (Bennett et al. 2012; Bravo et al. 2011; Cooper, Steiner & Brown 2009). The channel radius a of the $^{12}\text{C}+^{12}\text{C}$ channel is subject to a large uncertainty. The Coulomb penetration factor and the Wigner limit are highly dependent on this a value. Kanungo et al. (2016) derived a matter radius of 2.35 fm from the measurements of charge exchange reaction cross section, thus the channel radius for the $^{12}\text{C}+^{12}\text{C}$ fusion reaction is estimated to be simply double of a matter radius of single carbon nucleus, $a = 4.70$ fm. A model fitting of the astrophysical S -factor by Yakovlev et al. (2010) also suggests a channel radius as large as $a = 7.97$ fm. Fig. 1 therefore includes both cases, i.e. $a = 4.70$ fm and 7.97 fm. In this study, we adopt $a = 7.97$ fm because one of our goals is to put an upper limit on the resonance strength.

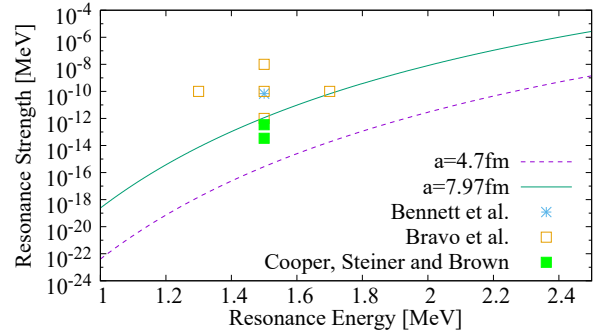


Figure 1. The resonance strength with $\theta^2 = 1$ (Wigner limit) as a function of the resonance energy E_R . The broken and solid lines are for the cases of $a = 4.70$ fm and 7.97 fm, respectively (Kanungo et al. 2016; Yakovlev et al. 2010). The total angular momentum of the resonance is assumed to be $J = 0$. The asterisk, and open and closed squares show the resonance parameters adopted in the previous works (Bennett et al. 2012; Bravo et al. 2011; Cooper, Steiner & Brown 2009).

One can find in Fig. 1 that the resonance strength in Bennett et al. (2012) and three of the resonances in Bravo et al. (2011) are excluded, two in Bravo et al. (2011) are marginally consistent with our upper limit, and those in Cooper, Steiner & Brown (2009) are consistent with the upper limit.

3 IMPLICATION FOR WD-WD MERGERS

3.1 Basic Scenarios of WD Binary Mergers

The evolution of WD binary mergers into SN Ia explosions or collapse to NSs depends on τ_C , τ_ν and τ_{dyn} , where τ_{dyn} is the typical dynamical timescale of the system. Given the energy generation rate of carbon burning ϵ_C (Blinnikov & KhoKhlov 1987) and the neutrino cooling rate ϵ_ν (Itoh et al. 1996), the timescales corresponding to these processes are $\tau_C = C_p T/\epsilon_C$, $\tau_\nu = C_p T/\epsilon_\nu$, where C_p is the specific heat. The fate of WD-WD binary mergers is illustrated in Fig. 2.

If the total mass is smaller than the Chandrasekhar mass M_{ch} , a massive white dwarf remains. Let us assume here that the total mass of the two WDs is larger than M_{ch} . If the secondary WD accretes gas materials violently onto the primary WD, carbon burning occurs dynamically and detonation propagates throughout the system, which leads to a SN Ia explosion. This occurs when $\tau_{\text{dyn}} > \tau_C$ and is called the violent merger (VM; Pakmor et al. 2010, 2012). If the detonation does not occur in the merger phase for $\tau_{\text{dyn}} < \tau_C$, a remnant that has a cold core, a hot envelope and an outer disk is formed. If the ignition condition for carbon burning $\epsilon_C > \epsilon_\nu$ or equivalently $\tau_C < \tau_\nu$ is satisfied in the envelope, a carbon burning front propagates through the core and converts the CO WD into an ONeMg one. Once the ONeMg WD forms, it cannot support the mass because of electron capture and it collapses into a NS. This scenario is referred to as the accretion induced collapse (AIC; Nomoto & Kondo 1991).

For $\tau_\nu < \tau_C$, the WD will explode as a SN Ia due to the

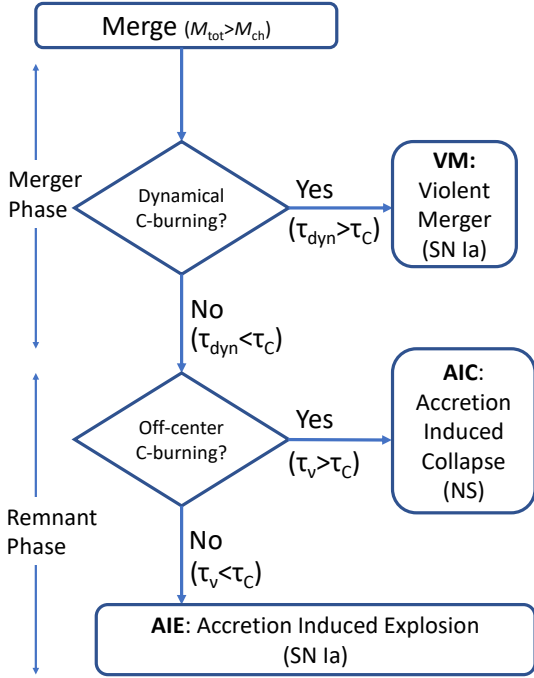


Figure 2. The standard scenario on the evolution of WD-WD binary mergers.

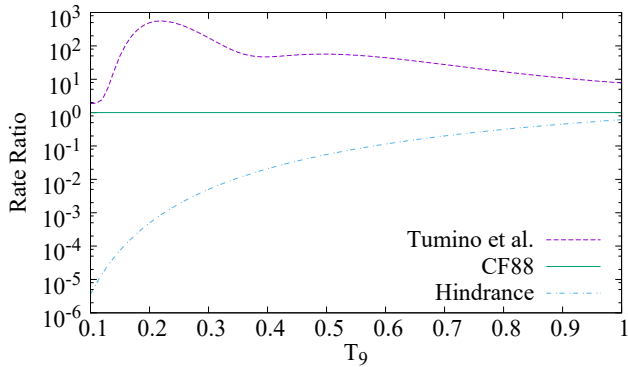


Figure 3. The $^{12}\text{C}+^{12}\text{C}$ reaction rate normalized by the CF88 rate.

high central density (namely, accretion induced explosion; AIE).

3.2 Ignition Condition of Carbon Burning

Tumino et al. (2018a) succeeded in measuring the cross sections below 2 MeV using the Trojan Horse Method (Tribble et al. 2014) with the three-body processes $^{12}\text{C}(^{14}\text{N}, \alpha^{20}\text{Ne})^2\text{H}$ and $^{12}\text{C}(^{14}\text{N}, p^{23}\text{Na})^2\text{H}$. Several resonances were found near the Gamow peak resulting in reaction rates roughly 25 times that of CF88 at $T = 5 \times 10^8$ K. The reaction rates as a function of the temperature are shown in Fig. 3 (purple broken line). On the other hand, Jiang et al. (2007) suggested that the S^* -factor can decrease in the low-energy region. This “hindrance” model is shown in the blue broken line in Fig. 3.

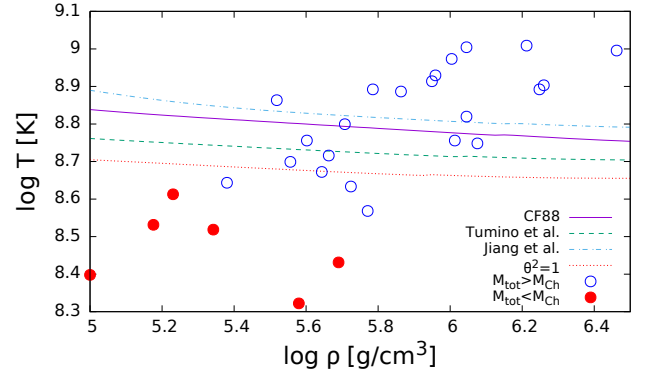


Figure 4. The ignition curve $\epsilon_{\text{C}} = \epsilon_{\nu}$ (i.e. $\tau_{\text{C}} = \tau_{\nu}$) for the C-burning rate with and without the resonance contribution. The ignition temperature with the experimental reaction rate (Tumino et al. 2018a) is drawn in the green line. The blue line shows the ignition temperature with the hindrance model (Jiang et al. 2007). The circles are calculated results of SPH simulations of Sato et al. (2015, 2016). The blue open points are for systems with $M_{\text{tot}} > 1.4M_{\odot}$ and the red closed points are for systems with $M_{\text{tot}} < 1.4M_{\odot}$.

The ignition curve, shown in Fig. 4., is defined to be the temperature and density at which the ignition condition, $\epsilon_{\text{C}} = \epsilon_{\nu}$, is satisfied. Here, θ^2 is the dimensionless reduced width (e.g. Clayton 1968) of an assumed Breit-Wigner resonance at a resonance energy of $E_{\text{R}} = 1.37$ MeV (Chiba & Kimura 2015), thus the $\theta^2 = 1$ corresponds to the theoretical lower limit of the ignition temperature. For this figure, the approximation of a narrow resonance is adopted. Also shown are the calculated results of smoothed particle hydrodynamics (SPH) simulations of WD mergers (Sato et al. 2015, 2016), which indicate the highest temperature observed in the simulation and the density at that point. The blue open and closed red circles in this figure represent the calculated results from various combinations of progenitor in the SPH simulations for systems of total mass with $M_{\text{tot}} > 1.4M_{\odot}$ and $M_{\text{tot}} < 1.4M_{\odot}$, respectively. The systems above the ignition curve will collapse to NSs, while those below the curve will explode as SNe Ia, if the total mass is larger than $M_{\text{ch}} \sim 1.4M_{\odot}$. Some of the systems which result in AIE using only the non-resonant CF88 rate evolve into the AIC eventually since including the resonance contribution lowers ignition temperature.

Secondary reactions contribute to energy generation in carbon burning. Blinnikov & KhoKhlov (1987), followed by Dan et al. (2014) and Sato et al. (2015), suggested an average Q -value, $Q_{\text{ave}} = 9.27$ MeV, assuming a branching ratio of 1/2 for the reactions $^{12}\text{C}(^{12}\text{C}, \alpha)^{20}\text{Ne}$ ($Q = 4.6$ MeV) and $^{12}\text{C}(^{12}\text{C}, \gamma)^{24}\text{Mg}$ ($Q = 13.9$ MeV). This assumption, however, should be revised using detailed reaction network calculations (Chamulak et al. 2008; Iliadis 2008). Iliadis (2008) performed a network calculation with constant temperature and density at $T_9 = 0.9$ and $\rho = 10^5$ g/cm 3 with initial composition of $X(^{12}\text{C}) = 0.25$, $X(^{16}\text{O}) = 0.73$, $X(^{20}\text{Ne}) = 0.01$ and $X(^{22}\text{Ne}) = 0.01$, which is analogous to the environments in the WD mergers. It was shown that the major secondary reactions are $^{23}\text{Na}(p, \alpha)^{20}\text{Ne}$ ($Q = 2.38$ MeV) and $^{16}\text{O}(\alpha, \gamma)^{20}\text{Ne}$ ($Q = 4.73$ MeV), which lead to the net reac-

tion of $2\times^{12}\text{C}+^{16}\text{O}\rightarrow 2\times^{20}\text{Ne}$ ($Q = 9.35$ MeV). This Q -value 9.35 MeV of the net reaction is so similar to the averaged Q_{ave} from [Blinnikov & KhoKhlov \(1987\)](#) that this difference does not practically affect the ignition condition. However, it is noted that the physical situation is different. [Chamulak et al. \(2008\)](#) also performed a network calculation with higher densities $\rho \geq 10^9$ g/cm³. It is desirable to use their effective Q -values for realistic burning processes near the center of WDs or the surface of NSs.

3.3 Fate of WD Binary Mergers

Fig. 5 shows the merger outcomes for the calculated results using the CF88 rate and the enhanced reaction rate by [Tumino et al. \(2018a\)](#). The masses of the primary and secondary WDs are denoted by M_1 and M_2 , respectively (i.e. $M_1 > M_2$). The difference between the results for the two rates is the shaded region in which mergers with $M_1 = 0.9M_{\odot}$ go to the AIC path for the case including the resonance, while they go to the AIE path for the non-resonant CF88 rate.

Combining these results with the mass distribution of single DA¹ WDs extracted from Data Release 4 of the Sloan Digital Sky Survey (SDSS) ([Kepler et al. 2007](#)), we can estimate a SN Ia rate which comes from the WD-WD mergers. [Badenes & Maoz \(2012\)](#) showed that the Galactic event rate of WD-WD mergers per unit stellar mass is estimated to be $1.4^{+3.4}_{-1.0} \times 10^{-13} M_{\odot}^{-1}\text{yr}^{-1}$ from spectroscopic data. The VM rate is $8.4^{+20.4}_{-6.0} \times 10^{-17} M_{\odot}^{-1}\text{yr}^{-1}$ and nearly independent of reaction rates because the critical temperature to cause the dynamical instability necessary for a VM is as high as $T_9 > 1.5$. However, the AIE rate changes depending on the resonance contribution. Its rate is $1.3^{+3.2}_{-0.92} \times 10^{-14} M_{\odot}^{-1}\text{yr}^{-1}$ for the non-resonant CF88 rate, while it decreases to $1.2^{+2.9}_{-0.85} \times 10^{-14} M_{\odot}^{-1}\text{yr}^{-1}$ for the rate plus resonance contribution, compared to the rate of SNe Ia in Sbc² galaxies with the stellar mass of the Milky Way is $\sim (1.1 \pm 0.2) \times 10^{-13} M_{\odot}^{-1}\text{yr}^{-1}$ ([Li et al. 2011](#)). WD-WD mergers account for only $\sim 12\%$ of SNe Ia for the case of the CF88 rate and the situation is almost the same for the [Tumino et al. \(2018a\)](#) rate. The result is summarized in Table 1 for several reaction rates.

Recently, [Maoz & Hallakoun \(2017\)](#) estimated the Galactic WD-WD merger rate as $(7 \pm 2) \times 10^{-13} M_{\odot}^{-1}\text{yr}^{-1}$ using spectroscopic data from the ESO-VLT SN Ia Progenitor Survey (SPY). This is ~ 5 times larger than the estimate of [Badenes & Maoz \(2012\)](#). Event rates calculated from [Maoz & Hallakoun \(2017\)](#) are summarized in Table 2. Using [Tumino et al. \(2018a\)](#) reaction rate, the DD scenario would be responsible for $\sim 55\%$ of the SNe Ia rate.

The NS birth rate has been estimated to be $10.8^{+7.0}_{-5.0}$ NSs/century, while the CCSN rate is estimated to be 1.9 ± 1.1 SNe/century from measurements of γ -ray from ²⁶Al ([Diehl et al. 2006](#); [Keane & Kramer 2008](#)), suggesting that the origin of NSs is supplemented by the AIC path of the WD mergers. The estimated AIC rate is tabulated in Table 1

¹ WDs can be classified by their optical spectra. DA is a class with strong hydrogen lines.

² Sbc is one of morphological classes of barred spiral galaxies, to which the Milky Way Galaxy is believed to belong.

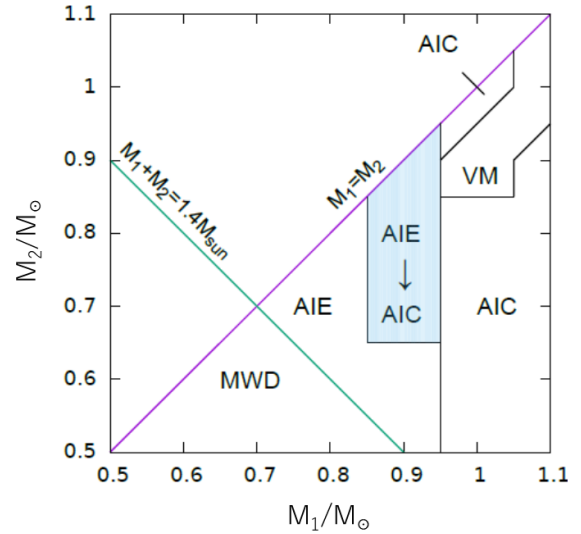


Figure 5. The outcome of the WD-WD mergers on the M_1 - M_2 parameter plane with the enhanced reaction rate of [Tumino et al. \(2018a\)](#). The colored area at $M_1 \sim 0.9M_{\odot}$ shows the systems which change their fate from AIE to AIC when the resonance is assumed. MWD is an abbreviation of massive white dwarfs.

and 2. The [Tumino et al. \(2018a\)](#) reaction rate can increase this rate by $\sim 20\%$. However, the enhanced AIC rate does not completely solve the birthrate problem of the NSs.

The astrophysical event rates are summarized in Fig. 6 as a function of θ^2 . In this figure, the resultant event rates with the [Tumino et al. \(2018a\)](#) reaction rate correspond to $\theta^2 \approx 0.1$.

The ignition temperature of carbon burning increases if the hindrance model ([Jiang et al. 2007](#)) is adopted, as shown in Fig. 4. This leads to a higher AIE rate of $1.4^{+3.4}_{-1.0} \times 10^{-14}/M_{\odot}/\text{yr}$ and a lower AIC rate of $3.6^{+8.7}_{-2.6} \times 10^{-15}/M_{\odot}/\text{yr}$ than those calculated with CF88, assuming the event rate of mergers of [Badenes & Maoz \(2012\)](#) (Table 1). If we use the event rate estimated by [Maoz & Hallakoun \(2017\)](#), these results become ~ 5 times larger (Table 2).

3.4 Model Uncertainties

Additional uncertainties are intrinsic to the hydrodynamic models. The SPH simulation in [Sato et al. \(2015\)](#) stops its calculations at the end of the early remnant phase. Subsequent evolution is dominated by physical viscosity, which has not been treated, despite the fact that the carbon burning can start in the viscous evolution phase ([Shen et al. 2012](#); [Schwab et al. 2012](#)). Therefore, some of the systems which go to the AIE path in this study may change their fate to the AIC path. Realistic simulations of mergers with viscosity are desirable to acquire the conclusive result.

[Sato et al. \(2015\)](#) checked the convergence of their results by changing the numerical resolution, reporting that the maximum temperature nearly converges in the remnant phase, while it gradually increases with higher resolutions in the merger phase. Hence the fate of some systems may change from AIC to VM if simulations for higher-resolution studies are carried out.

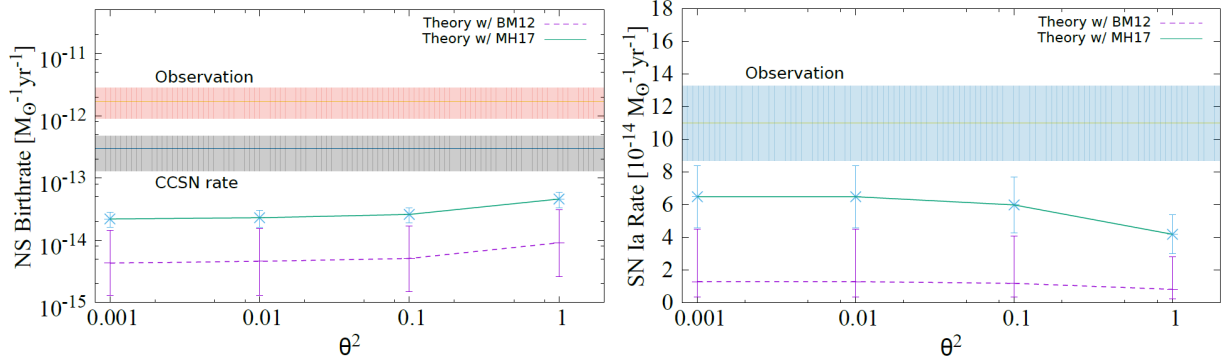


Figure 6. (Left) The birthrate of NSs. The bands show observational uncertainties. The points show the theoretical AIC rates with the WD-WD merger rates [Badenes & Maoz \(2012\)](#) (BM12) and [Maoz & Hallakoun \(2017\)](#) (MH17). (Right) The event rate of SNe Ia. The band show observational uncertainty.

Table 1. The event rates of the AIC, AIE and VM paths in units of $10^{-14} / M_{\odot} / \text{yr}$ and the ratio of NSs and SNe Ia that can be explained in each scenario. The Galactic WD-WD rate is from [Badenes & Maoz \(2012\)](#).

	AIC	AIE	VM	AIC/NS	(VM+AIE)/SNIa
CF88	$0.43^{+1.0}_{-0.30}$	$1.3^{+3.2}_{-2.92}$	$0.0084^{+0.0204}_{-0.0060}$	$0.0025^{+0.013}_{-0.0020}$	$0.12^{+0.40}_{-0.091}$
Tumino et al. (2018a)	$0.51^{+1.2}_{-0.36}$	$1.2^{+2.9}_{-0.85}$	$0.0084^{+0.0204}_{-0.0060}$	$0.0030^{+0.016}_{-0.0025}$	$0.11^{+0.36}_{-0.084}$
$\theta^2 = 1$	$0.91^{+2.2}_{-0.65}$	$0.83^{+2.0}_{-0.59}$	$0.0084^{+0.0204}_{-0.0060}$	$0.0054^{+0.029}_{-0.0045}$	$0.076^{+0.25}_{-0.058}$
Hindrance	$0.36^{+0.87}_{-0.26}$	$1.4^{+3.4}_{-1.0}$	$0.0084^{+0.0204}_{-0.0060}$	$0.0021^{+0.011}_{-0.0017}$	$0.13^{+0.42}_{-0.10}$

Table 2. Same as Table 1, but [Maoz & Hallakoun \(2017\)](#) is adopted as the WD-WD merger rate.

	AIC	AIE	VM	AIC/NS	(VM+AIE)/SNIa
CF88	2.2 ± 0.6	6.5 ± 1.9	0.042 ± 0.012	$0.013^{+0.018}_{-0.007}$	$0.60^{+0.37}_{-0.24}$
Tumino et al. (2018a)	2.6 ± 0.7	6.0 ± 1.7	0.042 ± 0.012	$0.015^{+0.021}_{-0.008}$	$0.55^{+0.34}_{-0.23}$
$\theta^2 = 1$	4.6 ± 1.3	4.2 ± 1.2	0.042 ± 0.012	$0.027^{+0.038}_{-0.015}$	$0.38^{+0.24}_{-0.15}$
Hindrance	1.8 ± 0.5	7.0 ± 2.0	0.042 ± 0.012	$0.011^{+0.013}_{-0.006}$	$0.64^{+0.39}_{-0.27}$

4 SUMMARY AND FUTURE PROSPECT

The low energy resonances in the $^{12}\text{C}+^{12}\text{C}$ fusion reaction were studied. Resonant reaction rates were applied to WD-WD binary mergers. The enhanced reaction rate results in a lower ignition temperature, leading to a higher probability of finding WD-WD mergers reaching the AIC. This could increase the birthrate of the Galactic NSs making the fraction of the WD mergers in the progenitors of SNe Ia smaller. Although this result favors a partial solution of the NS birthrate problem, the contribution of the DD scenario to SNe Ia is still largely subject to observational errors.

The result by [Tumino et al. \(2018a\)](#) significantly impacts a wide range of astrophysics, though the validity of this method is a subject of debate. [Mukhamedzhanov, Tang & Pang \(2018\)](#) pointed out that the Coulomb interaction is so large that the plane-wave approach used in [Tumino et al. \(2018a\)](#) could be questionable at the energies used in their experiment and that the *R*-matrix analysis should be reevaluated to account for identical bosons, etc. [Tumino et al. \(2018b\)](#) quickly replied counter discussion against [Mukhamedzhanov, Tang & Pang \(2018\)](#), but theoretical assumptions used in the data analysis are to be carefully studied. Therefore, both measurements of the low energy cross sections and theoretical analysis of the molecular resonances in the ^{24}Mg nuclear system are highly desirable to confirm the existence of the resonances and to determine the reso-

nance parameters E_R , Γ_{tot} , and partial decay widths, especially of the carbon channel Γ_C . The Laboratory for Underground Nuclear Astrophysics (LUNA; [Costantini et al. 2009](#)) is planning to measure the low energy cross sections down to the Gamow peak.

ACKNOWLEDGEMENTS

The authors thank Shigeru Kubono and Izumi Hachisu for helpful discussions. KM was supported by a grant from the Hayakawa Satio Fund awarded by the Astronomical Society of Japan. MAF was supported by the National Science Foundation under Grant No. PHY1712382. This work is supported by JSPS KAKENHI Grant Numbers JP15H03665 and JP17K05459.

REFERENCES

- Aguilera, E. F., Rosales, P., Martínez-Quiroz, E., et al. 2006, *Phys. Rev. C*, 73, 064601
 Badenes, C., & Maoz, D. 2012, *ApJ*, 749, L11
 Barrón-Palos, L., Aguilera, E. F., Aspiazua, J., et al. 2006, *NuPhA*, 779, 318
 Becker, H. W., Kettner, K. U., Rolfs, C., et al. 1981, *ZPhyA*, 303, 305

- Bennett, M. E., Hirschi, R., Pignatari, M., et al. 2012, *MNRAS*, 420, 3047
- Blinnikov, S. I., & KhoKhlov, A. M. 1987, *SvAL*, 13, 364
- Bravo, E., Piersanti, L., Domínguez, I., et al. 2011, *A&A*, 535, A114
- Caughlan, G. R., & Fowler, W. A. 1988, *ADNDT*, 40, 283
- Chamulak, D. A., Brown, E. F., Timmes, F. X., et al. 2008, *ApJ*, 677, 160
- Chiba, Y., & Kimura, M. 2015, *Phys. Rev. C*, 91, 061302
- Clayton, D. D. 1968, *Principles of Stellar Evolution and Nucleosynthesis* (University Of Chicago Press)
- Costantini, H., Formicola, A., Imbriani, G., et al. 2009, *RPPH*, 72, 086301
- Cooper, R. L., Steiner, A. W., & Brown, E. F. 2009, *ApJ*, 702, 660
- Dan, M., Rosswog, S., Brüggem, M., et al. 2014, *MNRAS*, 438, 14
- Diehl, R., Hallain, H., Kretschmer, K., et al. 2006, *Nature*, 439, 45
- Esbensen, H., Tang, X., & Jiang, C. L. 2011, *Phys. Rev. C*, 84, 064613
- High, M. D., & Cujec, B. 1977, *NPhA*, 282, 181
- Iben, I. Jr., & Tutukov, A. V. 1984, *ApJS*, 54, 335
- Iliadis, C. 2008, *Nuclear Physics of Stars* (Wiley-VCH)
- Imanishi, B. 1968, *PhLB*, 27, 267
- Itoh, N., Hayashi, H., Nishikawa, A., & Kohyama, Y. 1996, *ApJS*, 102, 411
- Jiang, C. L., Rehm, K. E., Back, B. B., et al. 2007, *Phys. Rev. C*, 75, 015803
- Kanungo, R. et al. 2016, *Phys. Rev. Lett.*, 117, 102501
- Kashiyama, K., Ioka, K., & Mészáros, P. 2013, *ApJ*, 776, L39
- Kawabata, T. et al. 2013, *J. Phys.: Conf. Ser.*, 436, 012009
- Keane, E. F., & Kramer, M. 2008, *MNRAS*, 391, 2009
- Kepler, S. O., Kleinman, S. J., Nitta, A., et al. 2007, *MNRAS*, 375, 1315
- Kettner, K. -U., Lorenz-Wirzba, H., Rolfs, C., et al. 1977, *Phys. Rev. Lett.*, 38, 337
- Levan, A. J., Wynn, G. A., Chapman, R., et al. 2006, *MNRAS*, 368, L1
- Li, W., Chornock, R., Leaman, J., et al. 2011, *MNRAS*, 412, 1473
- Maoz, D., & Hallakoun, N. 2017, *MNRAS*, 467, 1414
- Mazarakis, M. G., & Stephens, W. E. 1973, *Phys. Rev. C*, 7, 1280
- Mukhamedzhanov, A. M., Tang, X., and Pang, D. Y. 2018, arXiv: 1806.05921
- Munson, J. M., Norman, E. B., Burke, J. T., et al. 2017, *Phys. Rev. C*, 95, 015805
- Nomoto, K., & Kondo, Y. 1991, *ApJ*, 367, L19
- Notani, M., Esbensen, H., Fang, X., et al. 2012, *Phys. Rev. C*, 85, 014607
- Pakmor, R., Kromer, M., Röpke, F. K., et al. 2010, *Nature*, 463, 61
- Pakmor, R., Kromer, M., Taubenberger, S., et al. 2012, *ApJ*, 747, L10
- Patterson, J. R., Winkler, H., & Zaidins, C. S. 1969, *ApJ*, 157, 367
- Sato, Y., Nakasato, N., Tanikawa, A., et al. 2015, *ApJ*, 807, 105
- Sato, Y., Nakasato, N., Tanikawa, A., et al. 2016, *ApJ*, 821, 67
- Schwab, J., Shen, K. J., Quataert, E., et al. 2012, *MNRAS*, 427, 190
- Shen, K. J., Bildsten, L., Kasen, D., et al. 2012, *ApJ*, 748, 35
- Spillane, T., Raiola, F., Rolfs, C., et al. 2007, *Phys. Rev. Lett.*, 98, 122501
- Spinka, H., & Winkler, H. 1974, *NuPhA*, 233, 456
- Teichmann, T., & Wigner, E. P. 1952, *PhRv*, 87, 123
- Tribble, R. E., Bertulani, C. A., Cognata, M., et al. 2014, *RPPH*, 77, 106901
- Tumino, A., Spitaleri, C., La Cognata, M., et al. 2018, *Nature*, 557, 687
- Tumino, A., Spitaleri, C., La Cognata, M., et al. 2018, arXiv: 1807.06148
- Webbink, R. F. 1984, *ApJ*, 277, 355
- Yakovlev, D. G., Beard, M., Gasques, L. R., et al. 2010, *Phys. Rev. C*, 82, 044609
- Zickefoose, J. 2010, Ph.D. Thesis, University of Connecticut